TEMPORAL OCCURRENCE AND FORECASTING
OF LANDSLIDES IN THE EUROPEAN COMMUNITY
CONTRACT EPOCH N°90. 0025 (DTEE)

Final report. Oct.1993

Part I: Methodology (Reviews) for the Temporal Study of Landslides

DEBRIS FLOW MEASUREMENT METHODS

HARRY M. BLIJENBERG[1]

1 Department of Physical Geography, University of Utrecht, Netherlands

INTRODUCTION

Within the project 'Initiation And Frequency Of Debris Flows In An Alpine Environment' several types of investigation methods have been used. For the hydrological part of the project rainfall simulations were done, rainfall and runoff were measured, pF-samples were taken and analysed, and porosity of coarse debris was determined. Video recordings provided images of runoff events. Geodetic measurements formed the base for the production of digital terrain models used in GIS-based hydrologic and stability simulations. Strength characteristics of coarse debris were determined in the field, whereas those of flowing debris containing a high amount of fine material will be determined in the laboratory. Erosion pins provide data on temporal and spatial changes of surface level within a part of debris flow source area. Morphologic and hydrologic data of all debris flow source areas, as far as they can be safely investigated, will come from an inventarization and characterization of these areas. Photos contain additional qualitative and quantitative information on temporal changes. Rainfall records provide the base for a frequency analysis of debris flows over longer time scales. Finally, dating of debris flow deposits will provide the data needed to calibrate and validate the initiation-frequency model. These data may come from dendrochronological, lichenometrical and photographical sources and from archives.

HYDROLOGIC FIELD METHODS

As the amount of overland flow caused by rainfall is important for the initiation of a debris flow, some soil parameters describing its hydrologic characteristics have been determined. The main hydrologic parameters are the steady state infiltration capacity K and the sorptivity S of a soil. To determine these parameters a portable rainfall simulator has been used. It proved more practicle to take a portable rainfall simulator into the field than to take soil samples to the laboratory. This also had the advantage of causing little or no damage to the in-situ soil.

The rainfall simulator, shown in figure 1, covers a horizontal surface of $(24.5\pm0.5)*(24.5\pm0.5) = (600\pm17)$ cm². This means that 1 l water represents 16.7±0.5 mm of rainfall. Rain is produced from 49 holes on a 7*7 square grid with 3.5 cm between the holes. When a suitable location for a simulation was found, 4 rods were driven into the ground to provide a stable base for the simulator. A frame was fixed horizontally to the rods. Then the rainfall simulator was put in the frame, at 1.00-1.20 m above the soil surface.

In the rainfall simulator an air entry tube can be moved vertically. At the base of the air-entry tube atmospheric pressure is present, therefore adjusting it changes the fluid pressure at the rainfall simulator base and thus changes the flux through the holes. In this way the rainfall intensity can be controlled. This could be done by using a linear relation that was found between rainfall intensity and height difference between air entry level and rainfall simulator base (De Graaf et al., 1993):

$$i_r = 98.9 + 6.95h \qquad (1)$$

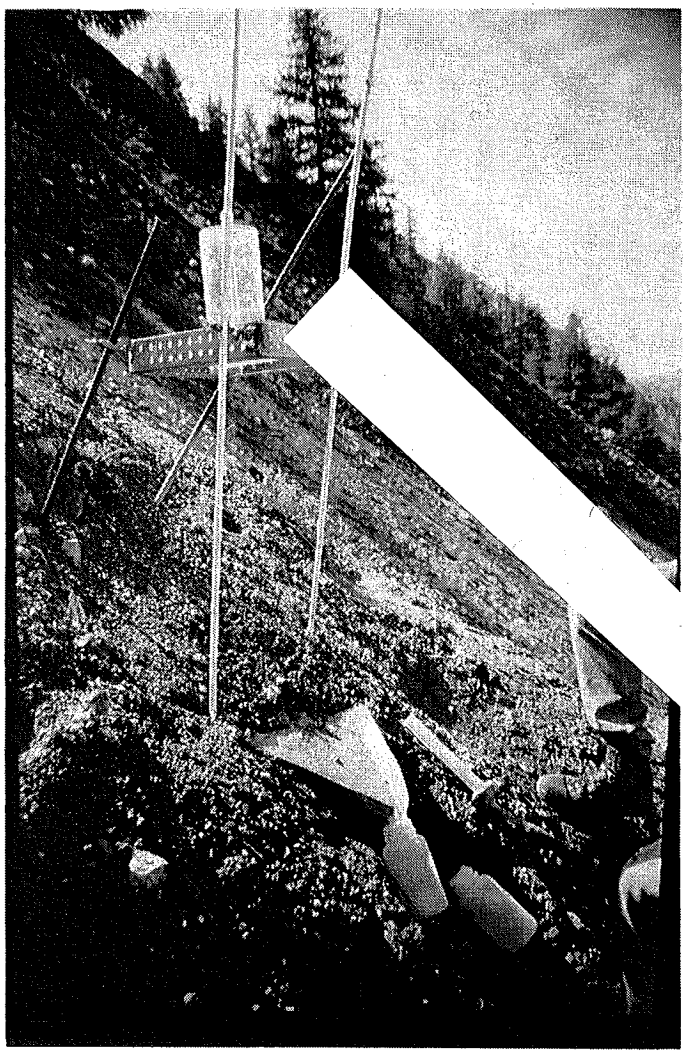

Figure 1 : The field portable rainfall simulator

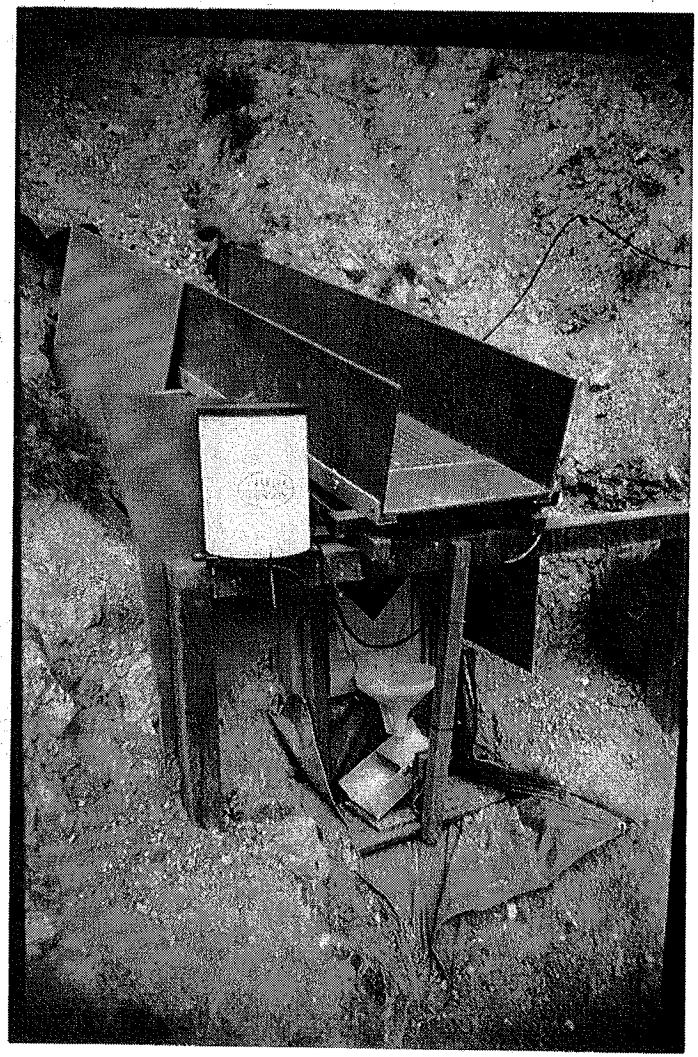

Figure 2 : The hydrologic monitoring installation in the Tête du Clot des Pastres debris flow source area.

where
i_r = rainfall intensity (mm/h)
h = vertical distance between base of air-entry tube and top of dripholes (mm)

During the period of testing however, it appeared that reading the water-level in the rainfall simulator at regular time-intervals provided a more accurate way to obtain rainfall intensities, as some variation in rainfall intensity remained unexplained by equation (1). With this rainfall simulator rainfall intensities of about 127 mm/h and more were possible. However, simulation of rain falling at lower intensities was desirable. Therefore the simulator was adapted to make testing at lower rainfall intensities possible. The adjustment consisted of narrowing the air entry tube, thus making air entry more difficult. Obviously, with the simulator set up like this, equation (1) is no longer valid and rainfall intensities were determined by reading water-level in the simulator at regular time-intervals. With rainfall intensities as low as 35 mm/h the adapted rainfall simulator made it possible to simulate naturally occurring rainfall intensities, which seldom exceed 150 mm/h in this area. The highest rainfall intensities used in the simulations were 290 mm/h. During simulations, rainfall intensity i_r and time-to-ponding t_p were determined. For some simulations overland flow was captured and intensity of overland flow i_{of} was determined. The mean slope gradient of the tested soil surface was measured using an Abney-level.

Two different evaluation methods were used. The first method used the overland flow intensity data. Once the overland flow intensity becomes constant, the difference between i_r and i_{of} is the steady state infiltration capacity K of a soil. The second method consisted of measuring t_p at different rainfall intensities for plots with similar humidity, texture, slope and micro-relief. From these measurements steady state infiltration capacity and sorptivity can be determined and an infiltration envelope can be constructed by connecting the ponding points (Imeson & Kwaad, 1982).

The rainfall simulator has some disadvantages. The small test surface causes relatively large boundary effects. The small fall distance causes raindrops to have less kinetic energy at impact than raindrops falling at final velocity. Imeson (1977) used a rainfall simulator with a large fall distance. Besides this, the uniform and large raindrops produced do not represent raindrop size distribution occurring in natural rain. A wire-netting used by Imeson (1977), intercepting the raindrops, produced a more realistic raindrop size distribution and improved his simulations even more. Still, it might be argued that in natural high-intensity rainstorms large raindrops have the major part of the kinetic energy. Also, the larger-than-natural raindrops produced by the rainfall simulator might compensate for the smaller-than-natural fall distance of the drops. Finally, such improvements would make the simulator less suitable for the difficult terrain that characterizes debris flow source areas in alpine environments.

In 1991 a hydrologic monitoring unit was installed in a part of a debris flow source area at an altitude of 2028 m. The unit, shown in figures 2 and 3, was installed in a gully in the debris flow source area on the eastern slope of the Tête du Clot des Pastres. It comprises a flume draining the upper 30 m of the gully, a grating in the flume separating coarse sediment from water and finer sediment, a tank with a

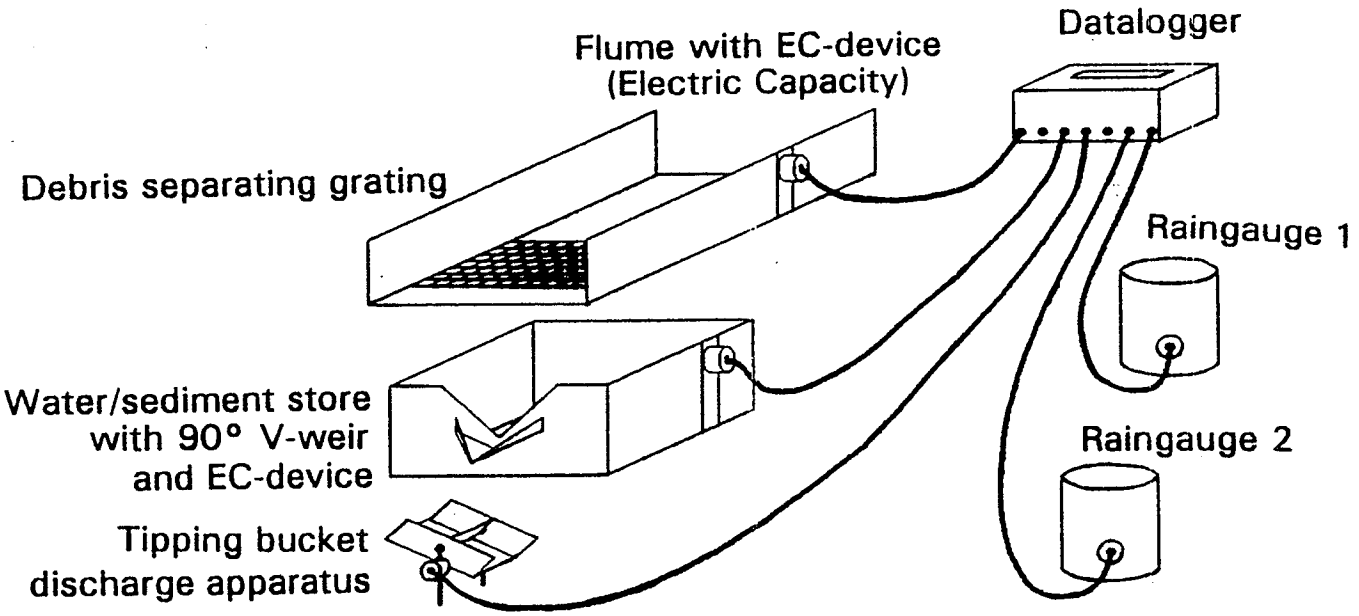

Figure 3 : The hydrologic monitoring installation: the 1991 setup.

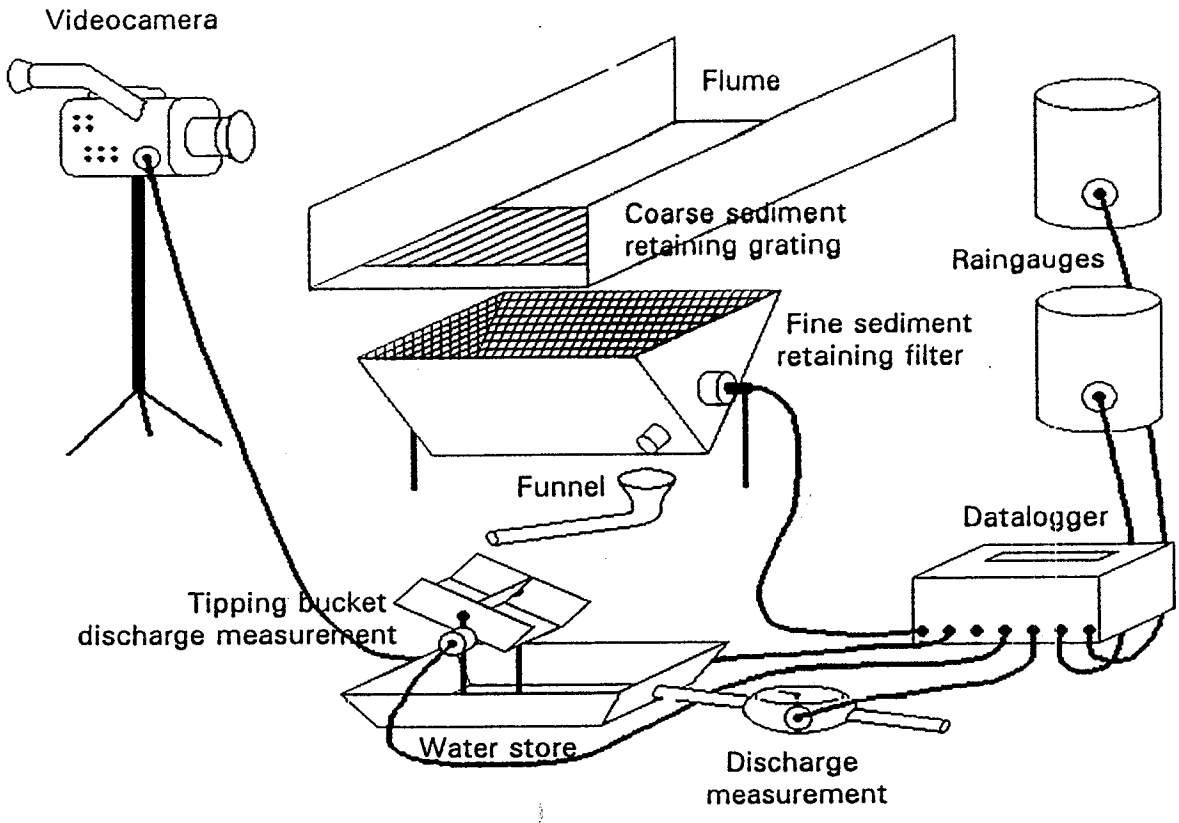

Figure 4: The hydrologic monitoring installation: the 1992/1993 setup.

water-level meter collecting the water and fine sediment, a tipping bucket discharge gauge and two raingauges. The raingauges, discharge gauge and water-level meter are connected to a datalogger, storing the registered values every minute.

The raingauges are both of tipping bucket type. They collect the rain fallen until about 0.2 mm of rain has fallen. Then the weight of the water causes the tipping bucket to tip over and give an electric signal to the datalogger, which counts the number of signals given by each raingauge in a minute. If the total number of tips of the two raingauges together in any one minute was more than one, the logger started storing date, time, rainfall, discharge and water-level until no more signals were given by the raingauges for 30 minutes. The raingauges were checked by a simple handheld raingauge that was read out regularly. It appeared that the raingauge installed 6 m from the flume on a ridge consistently produced more reliable results in 1992 than the raingauge installed next to the front of the flume. Therefore only the data from the raingauge on the ridge have been used for further analysis in 1992.

During a rainfall event overland flow might occur. Any overland flow reaching the installation was forced to flow through the flume. This flume, with a length of 200 cm, a width of 50 cm and a height of 28 cm, dipped 16° downslope. This was thought to be enough to let the material entering the flume continue its way after water was separated from it. Water and finer sediment were separated from the coarser sediment by a grating with square 2*2 cm^2 meshes that was mounted in the bottom of the flume. The material falling through the grating fell into a tank, where most of the finer sediment was captured. On one of the sides of the tank a plate was fixed, of which the electric capacity depended on the water-level in the tank. As water-level rose, it could reach the base of a 90° V-shaped weir that was cut into the front of the tank. The water flowing out of the tank was led to the tipping bucket discharge gauge, tipping every 0.5 l. This discharge gauge was designed to give reliable discharge measurements up to about 12 l/min. Higher discharges were to be calculated from an empirical relationship for a 90° V-shaped weir:

$$q = 1.34h^{2.48} \qquad (2)$$

where

q = discharge (l/s)

h = water-level above base of V-weir (cm)

After the 1991 campaign some limitations of the measurement unit became apparent. Firstly, the coarse debris transported to the flume did not continue its way when the water was separated from it at the grating. The material deposited on the grating blocked the way for any other material coming through the flume, which could quickly become filled up. Once the flume was filled up with sediment, new material reaching the flume would flow over the edges of the flume, not registered by the runoff measurement devices.

Sediment entering the tank would settle and after a high water-level had occurred in the tank, the sediment level would remain high. Capillary water in the sediment was measured by the electric capacity plate, irrespective of free water-level. This made the use of equation (2) impossible. Even when the sediment level in the tank was not above the base level of the V-weir, no unique relationship like equation (2) was found, which was probably caused by a change in the viscosity of

the fluid flowing from the tank as a result of a change in sediment content. Once the tank was filled up with sediment, any more sediment entering the tank would flow out to the tipping bucket discharge gauge, which finally was blocked by the sediment.

To overcome these problems, a part of the measurement unit was changed in 1992. The raingauges remained unchanged, but the logger was programmed to start storing rainfall and runoff data as soon as either of the two raingauges send a signal to the logger. The grating with square meshes in the flume was replaced by a grating made of bars 2 cm apart pointing in downslope direction. This grating was thought to present less friction to debris moving over it. A second sediment-removing wire-netting with 4 mm wide mazes was fixed under the grating, removing even more debris. The water and fine sediment finally fell into a tank with a fine maze, where most of the remaining debris was removed. Only the finest material (fine sand, silt, clay) and water were conducted from this tank to a box in which the water discharge was first gauged by a tipping bucket and then led through a conventional water discharge meter. Here the tipping bucket was again designed to give reliable results up to about 12 l/min; the conventional water-meter should registrate higher discharges. The sediment-tank was designed to tip over when filled with sediment, empty itself and then return to its original position within a few seconds. A video-camera was added to the installation to show how debris moved through the flume and whether or not the runoff measurements were reliable. Figure 4 shows the installation in summer 1992.

The renewed installation worked more reliable than the 1991 configuration, but still the grating would become blocked when debris moved over it and water was separated from it. The sediment-tank did not empty itself, but this proved to be no problem, as the tank never got full of sediment before it could be emptied manually. The video-camera showed that once the grating was blocked by debris, any more debris arriving at the flume would settle behind the blockage and finally water and sediment would flow over the edges of the flume.

In some debris flow source areas 100 cm^3 pF-samples were taken to determine bulk density, porosity and field water content of those parts where relatively fine material was present at the surface. Some pF-samples were taken to the laboratory to determine pF-curves. pF-samples were also taken at locations where rainfall simulations were carried out. The samples were taken near the rained surface before a rainfall simulation had taken place, and in the rained surface immediately after the simulation. This provided information on the changes in water content caused by the rain.

Problems encountered with pF-samples were disturbance of the material while sampling it, as even in relatively fine-grained material stones were often present. Another problem was caused by swelling and shrinking during respectively wetting and drying.

Porosity has also been measured in coarse debris. This was done by filling a bucket of known volume with coarse debris (containing little or no sand, silt or clay-sized material) and then fill the pores with water. Porosity is then simply calculated by:

$$\phi = V_w/V_b \qquad (3)$$

where

V_w = volume of water in bucket (l)
V_b = total volume of bucket (l)

The porosity measurements were done with debris of different mean grain size, sorting and packing. Loose packing was ensured by carefully putting material into the bucket without disturbing the material already present. Dense packing was brought about by shaking and beating the bucket.

Boundary effects caused by the bucket bottom and sides in these tests are very small, as appeared from tests in which porosity was measured for different filling levels of the bucket.

EROSION MEASUREMENTS

To get some idea of the amount of erosion occurring in the area drained by the hydrologic measurement unit, 51 erosion pins were installed at this site in 1992. They were driven vertically into the ground along three lines stretching from ridge to ridge perpendicular to the monitored gully. Within any one row the pins were installed at about 50cm from one another.

Measurement of the erosion pins consisted of measuring the distance of the top of the pin to the soil surface. Each pin was measured along four sides to obviate the effects caused by heaping up of material against the upslope part of the pin and of measurement location along the pin. The pins have been measured in july and october 1992 and in may 1993.

A problem encountered this year concerning the erosion pins was caused by displacement or disappearance of some of the erosion pins. Displacement had often caused the pins to stand oblique and in extreme cases the pins were pointing downslope.

DEBRIS STABILITY MEASUREMENTS

In 1991 a test was invented to measure the angle of internal friction of coarse, cohesionless debris in the field. The tests were to be carried out at those places where coarse, cohesionless debris had accumulated at surface slope angles near the angle of internal friction of the debris (slope angles >35°). Good testing sites were mainly found at the top of some scree slopes and in some gullies above scree slopes.

Originally the test was designed to function as presented in figure 5 a. In this test the static angle of internal friction φ_s would be directly measured. This had to be done by carefully digging away some debris on a slope of known surface slope angle. The material upslope would be on a local steeper slope and might fail at some point when too much material was taken away. The failure surface starts at the

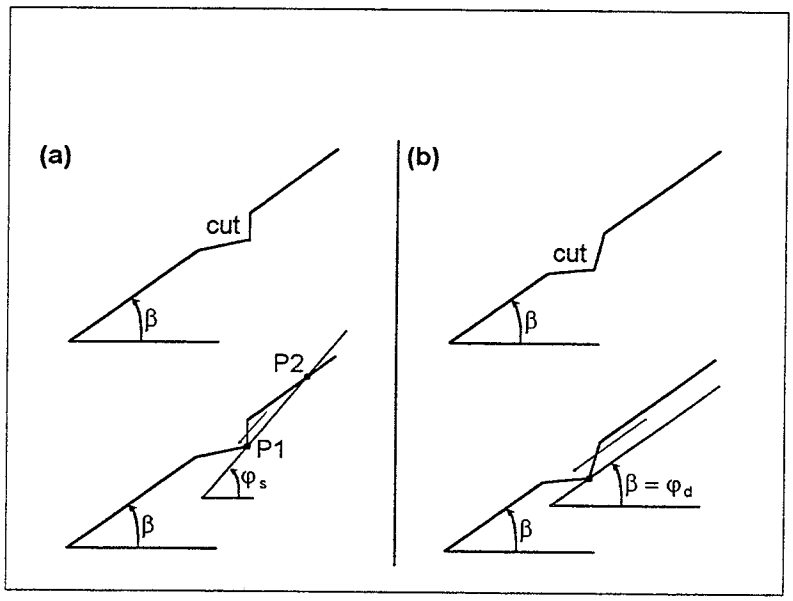

Figure 5: Test designs for determination of the angle of internal friction of coarse, cohesionless debris in the field.

downslope end of the local steeper slope P1 and ends at some point P2 upslope. If the depth of the dug-away material and the location of the end point of the failure surface are known, the angle of the failure surface can be calculated. When the mass that moves is large enough, boundary effects caused by single particles can be neglected and the angle of the failure surface equals the static angle of internal friction of the debris.

When the tests were carried out in the field in the summer of 1992, it proved to be impossible to find point P2. Often a few stones or small debris masses started to move and the impulse caused by their motion immediately initiated failure of more material. In these circumstances boundary effects were thought to have too much influence.

The test was slightly changed and became more simple to carry out and more reliable. When more material was dug away, a larger mass might start to move and continue to move slowly downslope for several decimetres or even metres. When such a mass moved slowly and gradually, without sudden changes in velocity, it was thought to be in dynamic equilibrium. If the dimensions of the moving mass were large enough compared to individual stone dimensions, the failure surface was supposed to be parallel to the surface as shown in figure 5 b. Therefore, measuring the surface angle of such a moving mass would give the dynamic angle of internal friction φ_d. The surface angle was measured by placing a 2 m long bar on the surface and measuring its inclination with an inclinometer (Abney-level or geologic compass). In order to avoid a large influence of boundary effects caused by a small ratio of individual stone dimensions to moving mass dimensions, the moving mass had to be at least 2 m long and at least 90% of the stones had to be smaller than 10 cm. The width of the mass had to be at least 10 times mean stone size and the depth of the failure surface at least 3 times mean stone size. Suitable debris therefore contained mainly stones < 5 cm, but the measured friction angles are believed to be valid for coarser debris as well.

With this test the dynamic angle of internal friction was determined for 5 different types of material: sandstone, flysch, limestone and two mixtures. For each type the test was done 50 times. This provided frequency distributions for each type which could be statistically compared. To characterize the debris types, for each type 100 stones were randomly picked and the principal axes of the stones measured. This might provide some idea of stone shape and stone size distribution and may be compared to dynamic angles of internal friction.

Debris material containing a high amount of fine-grained material (sand, silt and clay-sized particles) will be tested next autumn to determine the strength characteristics like cohesion, internal friction angle and viscosity. This will be done in the laboratory in a several metres long flume with a rough floor. The flume will have an adjustable slope angle. The strength characteristics will be determined for different water- and/or clay contents. The material that will be used for the tests was taken from a debris flow deposit.

MAPPING METHODS

Two debris flow source areas were accurately surveyed in 1991 by means of a theodolite and a distance-meter. In 1992 the area drained by the hydrologic

monitoring unit was surveyed in even more detail. Measurement points were as much as possible chosen along characteristic lines like ridges, gullies and rills. All the points along a (part of) such a characteristic line were called a 'measurement series'. By making sure that between any two adjacent points within a measurement series the slope segment was straight, more 'known' points could be generated along these series by linear interpolation.

With 150-300 measured points in each area and even more generated by linear interpolation, the datapoints on an irregular grid were interpolated to datapoints on regular grids using a kriging-based interpolation technique with the software package SURFER. The digital terrain model (DTM) produced by this program was used to produce contour maps of the debris flow source areas and was also used as a base map for hydrologic simulations.

As it appeared to be impossible to survey all debris flow source areas in the Bachelard valley by means of theodolite and distance-meter, this summer an attempt is made to inventarize and characterize all debris flow source areas by estimating, and where possible, measuring parameters describing the morphologic and hydrologic characteristics of the source areas. Among these are parameters concerning source area dimension, steepness and shape, amount of gullies, gully dimensions, vegetation cover and material at the surface.

PHOTOGRAPHIC ANALYSIS AND VIDEO RECORDINGS

Since 1991 several hundreds of photos have been taken of debris flows and their source areas. Many of these are stereo-pairs, and some locations have been regularly (once or twice a year) photographed. These photos make qualitative comparisons possible, and sometimes quantitative data can be obtained from the photos. Especially the temporal changes over the last few years can be derived from the photos, among which are new debris flow deposits. Such photos have not only been taken in the Bachelard valley, but in several other areas (Riou Bourdoux basin, Parpaillon valley) as well.

In 1992 a video camera was installed at the Tête du Clot des Pastres monitoring site near the hydrologic measurement unit. This camera has provided visual data on the reliability of the hydrologic monitoring unit in 1992. In the future it must provide data on debris flow initiation characteristics and debris flow movement.

DATING METHODS

Dating of existing debris flow deposits will provide a check on the initiation-frequency model of debris flows. Dendrochronological and lichenometrical methods, described in more detail elsewhere, will be used, as well as photo-analysis and archives.

COMPUTER SIMULATION TECHNIQUES

Using a DTM and the data obtained from hydrological measurements and rainfall simulations, a hydrological simulation was performed on a PC using the module WATERSHED of the PC-RASTER software package. Also some simple hydrological models, like the exponential storage model, will be tested for their usefulness for forecasting runoff from source areas that have not been surveyed geodetically.

Once initiation conditions for debris flows are known, debris flow initiation can be simulated as well on a PC. Combining rainfall record data, hydrologic simulations and debris flow initiation conditions, debris flow frequency may be simulated and can be checked against dated debris flow deposits.

REFERENCES

DE GRAAF P.J., DE RUITER J.F. & VAN TETERING A.A.A. (1993). *De initiatie van puinstromen. Een onderzoek in het Bachelarddal, Alpes de Haute-Provence, Frankrijk.* Unpublished report Utrecht University, Department of Physical Geography, 119 pp. (in dutch).

IMESON A.C. (1977). *A simple field portable rainfall simulator for difficult terrain.* Earth Surface Processes, vol. 2, pp.431-436.

IMESON A.C. & KWAAD F.J.P.M. (1982). *Field measurements of infiltration in the Rif Mountains of Northern Morocco.* Studia Geomorphologica Carpatho-Balcanica, nr. 15, pp. 19-30.